



Publication Year	2008
Acceptance in OA @INAF	2023-01-24T13:12:07Z
Title	Detection of C3O in the low-mass protostar Elias 18
Authors	PALUMBO, Maria Elisabetta; LETO, PAOLO; Siringo, C.; TRIGILIO, CORRADO
DOI	10.1086/591017
Handle	http://hdl.handle.net/20.500.12386/33036
Journal	THE ASTROPHYSICAL JOURNAL
Number	685

Detection of C₃O in the low-mass protostar Elias 18

M. E. Palumbo

INAF-Osservatorio Astrofisico di Catania, I-95123 Catania, Italy

mepalumbo@oact.inaf.it

P. Leto

INAF-Istituto di Radioastronomia, Sez. Noto, Italy

C. Siringo

Università degli Studi di Catania, Dipartimento di Fisica ed Astronomia, Catania, Italy

and

C. Trigilio

INAF-Osservatorio Astrofisico di Catania, I-95123 Catania, Italy

ABSTRACT

We have performed new laboratory experiments which gave us the possibility to obtain an estimate of the amount of carbon chain oxides (namely C₃O₂, C₂O, and C₃O) formed after irradiation (with 200 keV protons) of pure CO ice, at 16 K. The analysis of laboratory data indicates that in dense molecular clouds, when high CO depletion occurs, an amount of carbon chain oxides as high as $2\text{--}3 \times 10^{-3}$ with respect to gas phase carbon monoxide can be formed after ion irradiation of icy grain mantles. Then we have searched for gas phase C₂O and C₃O towards ten low-mass young stellar objects. Among these we have detected the C₃O line at 38486.891 MHz towards the low-mass protostar Elias 18. On the basis of the laboratory results we suggest that in dense molecular clouds gas phase carbon chain oxides are formed in the solid phase after cosmic ion irradiation of CO-rich icy mantles and released to the gas phase after desorption of icy mantles. We expect that the Atacama Large Millimeter Array (ALMA), thanks to its high sensitivity and resolution, will increase the number of carbon chain oxides detected in dense molecular clouds.

Subject headings: astrochemistry — ISM: molecules — ISM: individual (Elias 18) — methods: laboratory

1. Introduction

One of the main open questions in astrochemistry is the relation between solid phase and gas phase chemistry in dense molecular clouds. In fact in these regions ice mantles form on silicatic and carbonaceous grains after both direct freeze out of gas phase species and grain surface reactions. The presence of icy grain mantles is indirectly deduced from depletion of gas phase species and directly observed in the infrared from absorption features, attributed to vibrational modes of solid phase molecules, superposed to the background stellar spectrum. Icy grain mantles have been detected both in quiescent regions and in star forming regions. In both environments these suffer from energetic processing due to cosmic ions and UV photons. Ion and UV irradiation cause a modification of the structure and of the chemical composition of grain mantles, that is the formation of molecular species not present in the original ice. After desorption of icy mantles molecular species are released to the gas phase which could be enriched by species formed in the solid phase.

Former laboratory experiments have shown that carbon chain oxides (e.g., C_2O , C_3O , C_3O_2 , C_4O , C_5O_2 , C_7O_2) are formed after ion irradiation and UV photolysis of CO-rich ice mixtures (e.g., Strazzulla et al. 1997; Gerakines & Moore 2001; Trottier & Brooks 2004; Loeffler et al. 2005) along with carbon dioxide (CO_2) which is the most abundant molecule formed (e.g., Gerakines et al. 1996; Loeffler et al. 2005).

Carbon chain oxides, namely dicarbon monoxide (C_2O) and tricarbon monoxide (C_3O) have been detected in the molecular cloud TMC-1 towards the cyanopolyyne peak (hereinafter TMC-1CP) and it has been estimated that fractional abundance of C_2O is about 6×10^{-11} and that of C_3O is about 1.4×10^{-10} . These abundances have been explained by ion-molecule gas phase reactions (Matthews et al. 1984; Brown et al. 1985; Ohishi et al. 2001; Kaifu et al. 2004). C_3O has also been extensively searched for (Matthews et al. 1984; Brown et al. 1985) towards other objects, some of which are rich molecular-line sources and which together encompass a wide range of physical conditions. However C_3O was not detected in these regions and only upper limits have been estimated. Recently C_3O (Tenenbaum et al. 2006) as well as other O-bearing species, such as H_2O (Melnick et al. 2001; Hasegawa et al. 2006), OH (Ford et al. 2003), and H_2CO (Ford et al. 2004), have been detected towards the carbon star IRC +10216. This is an asymptotic giant branch star. O-bearing molecules are not expected in carbon stars since the bulk of available oxygen is contained in CO. In order to explain these observations it has been suggested that the increase in the star luminosity is causing the evaporation of orbiting icy bodies (Melnick et al. 2001). Alternatively it has been suggested that gas-phase oxygen-rich chemistry is occurring in the outer shell of the star (Tenenbaum et al. 2006).

Here we discuss new laboratory experiments which confirm the formation of carbon

chain oxides after ion irradiation of CO ice at low temperature and give us the possibility to obtain a quantitative estimate of the amount of carbon chain oxides formed with respect to initial carbon monoxide (Section 2). We present the new detection of the C_3O line at 38486.891 MHz towards the low-mass protostar Elias 18 and we confirm the detection of the same line towards TMC-1CP as already reported by Kaifu et al. (2004) (Section 3). On the basis of our laboratory results we suggest that gas phase carbon chain oxides in dense molecular clouds are actually formed in the solid phase after ion irradiation of CO-rich icy grain mantles and released to the gas phase after desorption of icy mantles (Section 4).

2. Experimental results

Experiments have been performed in the Laboratory for Experimental Astrophysics (INAF - Catania Astrophysical Observatory, Italy). A detailed description of the experimental set up can be found elsewhere (e.g., Strazzulla et al. 2001; Baratta et al. 2002; Palumbo et al. 2004). CO icy samples have been prepared on a cold substrate (16 K) in a vacuum chamber ($P=10^{-7}$ mbar) and then irradiated with 200 keV H^+ ions. Mid-IR transmission spectra (2.5-25 μm ; 4000-400 cm^{-1}) have been taken before, during and after irradiation. Different CO icy samples have been irradiated and the highest ion fluence was 1.5×10^{15} ions cm^{-2} . Figure 1 shows the spectrum of pure carbon monoxide in the 2450-1950 cm^{-1} (4.08-5.1 μm) spectral range at 16 K after irradiation with 200 keV H^+ ions (fluence equal to 1.25×10^{14} ions cm^{-2}). It is evident that after irradiation several absorption features are present which indicate the formation of molecular species not present in the original ice sample. In Figure 1 the intense CO band at about 2139 cm^{-1} (4.67 μm) and the CO_2 band at about 2343 cm^{-1} (4.27 μm) are out of scale. Main carbon chain oxides bands formed after irradiation are labeled. In Table 1 the peak position of most intense bands is reported along with their identification which is based also on the results presented by Trottier & Brooks (2004). A few features listed in Table 1 still remain unidentified and further laboratory experiments will be necessary for their identification.

Figure 2 shows the column density of carbon suboxide (C_3O_2), tricarbon monoxide (C_3O), and dicarbon monoxide (C_2O) with respect to initial carbon monoxide as a function of ion fluence after irradiation of CO ice at 16 K. Column density of C_3O_2 has been obtained from the band at 2398 cm^{-1} using the integrated absorbance value of 0.8×10^{-17} cm molecule $^{-1}$ given by Gerakines & Moore (2001). The column density of C_3O and C_2O have been obtained from the bands at 2247 cm^{-1} and 1989 cm^{-1} respectively. We note that the 2247 cm^{-1} band is superposed to the broader band at about 2242 cm^{-1} due to C_3O_2 . In order to estimate the integrated intensity (area) of this band we have considered a linear baseline

between 2246.7 and 2249.6 cm^{-1} . Given that the integrated absorbance of bands due to C_3O and C_2O has not been measured we have assumed a value of 1×10^{-17} cm molecule^{-1} for both bands. In fact this value is close to the average value measured for the absorption bands of many molecules (e.g., Mulas et al. 1998; Kerkhof et al. 1999; Bennett et al. 2004). The initial column density of carbon monoxide (the 2140 cm^{-1} band being saturated) has been measured from the interference curve given by a He-Ne laser beam reflected both by the vacuum-film and film-substrate interfaces (e.g., Baratta & Palumbo 1998) during accretion of the ice sample. An ice density equal to 0.8 g cm^{-3} (Loeffler et al. 2005) was used to obtain the column density value. The ratio of the column density of each species relative to the initial CO column density as a function of ion fluence has been fitted with the exponential curve $y = A(1 - e^{-\sigma\Phi})$ where Φ is the ion fluence (ions cm^{-2}), σ is the process cross section (cm^2) and A is the asymptotic value of the column density ratio. The σ and A values obtained for each species are reported in Fig. 2. In the case of C_3O_2 only data points obtained at ion fluence lower than 1.25×10^{14} ions cm^{-2} have been considered in the fitting procedure. In fact we noted that at higher fluence the column density of carbon suboxide decreases indicating that this species is destroyed after further irradiation. This also occurs to dicarbon monoxide and tricarbon monoxide at fluences higher than those given in Fig. 2. This effect has in fact already been observed for species formed after ion irradiation of other ice samples (e.g., Baratta et al. 2002). As discussed in details in Section 4, the top x-axis in Fig. 2 gives an estimation of the time (years) necessary to obtain on interstellar ices the same effects observed in laboratory. After irradiation was completed ice samples have been warmed up and spectra have been taken at 25, 40, 50, 60, 70 and 80 K. The spectrum at 25 K is almost indistinguishable from that taken at 16 K. Spectra taken at 16, 40, 50 and 80 K are shown in Fig. 3. It is evident that the intensity of absorption bands due to CO and carbon chain oxides rapidly decreases after warm up and that these are not detectable at about 80 K. On the other hand the bands due to carbon dioxide are present in the spectra at higher temperatures. This indicates that volatile species such as CO and carbon chain oxides sublime. Finally it is worth mentioning that carbon chain oxides are not formed after ion irradiation of O-rich ice samples such as $\text{CO}_2:\text{CO}$ and $\text{H}_2\text{O}:\text{CO}$ mixtures (Strazzulla et al. 1997).

3. Observations

Radio observations have been performed in 2006 September 6-12 with the 32-m radiotelescope in Noto (Italy). Sources observed are listed in Table 2. The telescope has an active surface system that compensates the gravitational deformation of the primary mirror making observations at high frequencies also possible. This new antenna set up, together with the

favorable weather conditions, allow to operate with good performance at high frequencies.

The observations have been carried out using the 22 GHz and the new 43 GHz (that can be tuned in the 38-47 GHz range) receivers. The beam size of the telescope (HPBW) was about 115'' at 22 GHz and 54'' at 43 GHz, the system noise temperature (including atmospheric noise and antenna ohmic losses) is about 90-120 K at zenith depending on weather conditions. The aperture efficiency of the telescope was about 0.28 at 43 GHz and 0.44 at 22 GHz. A duty cycle of 5 min integration on source and 5 min off source was used. Total integration time for each source is reported in Table 3.

The spectra have been acquired with the ARCOS autocorrelator (Comoretto et al. 1990) in beam switch mode; two spectra, one for each polarization, have been acquired simultaneously. Each spectrum has a bandwidth of 20 MHz, with a spectral resolution of 37 kHz, corresponding to a velocity resolution of 0.27 and 0.53 km s⁻¹ at 43 and 22 GHz respectively. The determination of the antenna efficiency as a function of the elevation has been performed by observing the flux calibrators 3C286, 3C123 and NGC7027. The spectra were reduced by using the software XSpetto for the on-off difference then software CLASS for the baseline subtraction and temperature calibration. The antenna temperature has been corrected to account for the variation of the effective area of the telescope as a function of elevation. Then all spectra have been averaged.

We have searched for the C₂O lines at 22258.181 MHz and 45826.706 MHz and the C₃O line at 38486.891 MHz towards the low-mass young stellar objects listed in Table 2. Our sample also includes TMC-1CP where the above lines have already been detected (Matthews et al. 1984; Brown et al. 1985; Ohishi et al. 2001; Kaifu et al. 2004). Figure 4 shows the C₃O line at 38486.891 MHz towards TMC-1CP. This detection confirms the previous results. We have not been able to confirm the detection of C₂O towards TMC-1CP as reported by Ohishi et al. (2001) and Kaifu et al. (2004) probably due to the low S/N ratio of our measurements. Figure 5 shows the C₃O line at 38486.891 MHz towards Elias 18. The peak intensity of the line is 0.031 K (S/N=4.4 with rms = 0.007 K). Rms for all the sources of our sample are given in Table 3. Fitting the line profile with a gaussian curve, we have measured that the integrated intensity of the line observed towards TMC-1CP is 0.039±0.008 K km s⁻¹ and towards Elias 18 is 0.025±0.005 K km s⁻¹. In the hypothesis that the source fills the antenna beam, assuming that the line is optically thin, using T_{ex}=20 K, μ(C₃O)=2.39 D, and B₀=4810.885 MHz (Brown et al. 1983), following the procedure described by Goldsmith & Langer (1999), we have estimated that C₃O column density is 8±2×10¹¹ molecules cm⁻² towards TMC-1CP and 5.2±1.3×10¹¹ molecules cm⁻² towards Elias 18. The value of the C₃O column density towards TMC-1CP we have found is lower than the value (1.4±0.4×10¹² molecules cm⁻²) reported by Matthews et al. (1984)

and Brown et al. (1985), however we believe that within the uncertainties of the estimation these values are comparable. Assuming $N(\text{H}_2) \simeq 1 \times 10^{22}$ molecules cm^{-2} (Guelin et al. 1982), we obtain an abundance of C_3O w.r.t. hydrogen of about 10^{-11} .

4. Discussion

Observations have shown that in dense molecular clouds the fractional abundance of carbon chain oxides (namely C_2O and C_3O) is of the order of 10^{-11} - 10^{-10} (Matthews et al. 1984; Brown et al. 1985; Ohishi et al. 2001; Kaifu et al. 2004, this work). In these regions the fractional abundance of CO is of the order of 10^{-4} then the abundance of carbon chain oxides with respect to CO values about 10^{-7} - 10^{-6} . Laboratory experiments here presented indicate that after ion irradiation of pure CO ice at 16 K the amount of carbon chain oxides formed is of the order of $2\text{-}3 \times 10^{-3}$ with respect to initial CO (Figure 2). In order to estimate the time necessary to obtain in dense molecular clouds the effects observed in the laboratory we consider the approximation of effective monoenergetic 1 MeV protons and assume that in dense interstellar regions the 1 MeV proton flux is equal to 1 proton $\text{cm}^{-2} \text{s}^{-1}$ (see Mennella et al. (2003) for a detailed discussion). However our experimental results were obtained using 200 keV protons. Thus in order to extrapolate the laboratory results to the interstellar medium conditions we assume that they scale with the stopping power (S, energy loss per unit path length) of impinging ions. Using the TRIM code (Ziegler 2003) we have estimated that for protons $S(200\text{keV})/S(1\text{MeV})$ is 3.8 in the case of pure CO ice. With these hypotheses in mind we have indicated in Fig. 2 timescale axis (top x-axis), which gives an estimation of the time (years) necessary to obtain the effects, observed in laboratory, on interstellar ices. Thus if we assume high CO depletion and that the carbon chain oxides/CO column density ratio obtained in the solid phase after ion irradiation is maintained in the gas phase after desorption of icy grain mantles, then from the exponential equation used to fit the data, we obtain that about 10^3 years would be necessary to form the observed column density of carbon chain oxides. As we will discuss below, this time is much shorter than the evolution time scale of dense clouds, thus the observed gas phase abundance of carbon chain oxides could be easily reached even if carbon monoxide is not completely depleted and/or only partial desorption of icy grain mantles takes place.

Towards all the young stellar objects observed in this work, the solid CO absorption band at $4.67 \mu\text{m}$ has been detected (e.g., Kerr et al. 1993; Chiar et al. 1994, 1995; Teixeira et al. 1998) along with the $3 \mu\text{m}$ band due to water ice which is the most abundant solid phase species along these lines of sight. However, recently, a detailed study of the solid CO band profile observed towards a large sample of low mass embedded objects (Pontoppidan et al.

2003) has shown that typical lines of sight have 60-90% of the solid CO in a pure or nearly pure form, suggesting that interstellar ices are best represented by a layered model rather than a mixed ice (e.g., Fraser et al. 2004). The presence of solid CO towards TMC-1CP has never been reported. In Taurus Molecular Cloud a threshold extinction $A_{th} \sim 6$ mag is required for CO ice detection (Chiar et al. 1995). Gas-phase models use $A_V=10$ mag in TMC-1 cores (e.g., Park et al. 2006) while $A_V=32$ mag towards TMC-1A (Teixeira & Emerson 1999) thus it seems reasonable to assume that CO ice is also present along the line of sight of TMC-1CP.

Elias 18 resides in a part of the Taurus molecular cloud known as Heiles cloud 2 (HCL2) where low-mass star formation is active. It is a highly obscured object ($A_V \sim 15$ -19 mag) and it has been suggested (Tegler et al. 1995) that it is in transition between an embedded young stellar object and an exposed T Tauri star. The IR spectral energy distribution (SED) for this source is typical of a class II or “flat-spectrum” YSO with significant optical extinction (Elias 1978). Recent observations indicate that Elias 18 has a circumstellar disk oriented close to edge-on and that most of the CO in the disk is incorporated in icy mantles on dust grains, i.e. high depletion is observed (Shuping et al. 2001). Mid-IR observations towards Elias 18 show the presence of both the solid CO and CO₂ absorption bands (e.g., Tielens et al. 1991; Chiar et al. 1995; Nummelin et al. 2001). The comparison between observations relative to solid CO and laboratory spectra indicates that different ice mixtures can equally well reproduce the observed band profile (Palumbo & Strazzulla 1993; Chiar et al. 1995, 1998). However all the fits indicate that a comparable amount of solid CO is in the nonpolar (i.e., CO-rich) and polar (i.e., H₂O-rich) components. Among the fits obtained, it has been shown that the nonpolar component can be reproduced by the spectrum of ion irradiated pure CO ice (and this is compatible with the hypothesis that CO-rich icy mantles are present along the line of sight in order to form carbon chain oxides) and the polar component can be reproduced by the spectrum of CO formed after ion irradiation of a H₂O:CH₃OH ice mixture (Palumbo & Strazzulla 1993). Detection of the stretching mode band of solid CO₂ towards Elias 18 and the comparison of the observed band profile with laboratory spectra have been reported by Nummelin et al. (2001). However, as discussed by Ehrenfreund et al. (1997); Gerakines et al. (1999); Ioppolo et al. (2008), the profile of the stretching mode band does not strongly depends on the ice mixture and cannot be used to constrain the ice composition along the line of sight.

TMC-1CP is a dense core in the TMC-1 cold dark cloud. Based on gas phase observations and chemical evolution models it has been deduced that its age is about 10^5 years and the density is $n_H = 2 \times 10^4 \text{ cm}^{-3}$ (Park et al. 2006). Thus the gas would take $10^9/n_H = 5 \times 10^4$ years to condense on grains (Tielens & Allamandola 1987). The presence of gas phase species implies that desorption processes, such as photodesorption, grain-grain collisions,

cosmic ray induced desorption and turbulence, compete with mantle accretion in this region (Boland & de Jong 1982; Hasegawa & Herbst 1993; Bringa & Johnson 2004).

Thus detection of C_3O towards these lines of sight is compatible with the hypothesis that this molecular species is formed in the solid phase and released to the gas phase when desorption of icy mantles takes place.

The results here discussed do not exclude that carbon chain oxides are also formed after gas phase reactions in dense molecular clouds. Furthermore we are aware that further observational data are necessary to confirm these results. In fact we plan to search for carbon chain oxides towards other sources in particular hot corinos in Class 0 low mass protostellar objects where evidence of ice mantle evaporation has been reported (Bottinelli et al. 2007).

One of the mysteries of interstellar chemistry is the mechanism regulating the balance between gas phase and solid phase species. Carbon chain oxides could be key molecules in this field and thanks to its high sensitivity and resolution the Atacama Large Millimeter Array (ALMA) will give important results increasing the number of detected features in a larger sample of molecular clouds.

Finally, as far as we know, the detection of C_2O and C_3O in comets has never been reported. However comets suffer from heavy ion irradiation (Strazzulla & Johnson 1991) and CO is abundant in these objects thus we expect that carbon chain oxides are present in comets too. In fact a tentative detection of carbon suboxide (C_3O_2) in comet Halley has been reported (Huntress et al. 1991; Crovisier et al. 1991). A firm detection of carbon chain oxides in comets could also be used to support the hypothesis that the presence of O-bearing species, and in particular C_3O , in carbon stars, such as IRC +10216, is due to sublimation of orbiting icy bodies as suggested by Melnick et al. (2001).

We would like to thank F. Spinella for his technical support during laboratory experiments, C. Contavalle and C. Nocita for their assistance during observations at Noto. This research has been financially supported by INAF and MIUR research contracts.

REFERENCES

- Baratta, G. A., & Palumbo, M. E. 1998, *J. Opt. Soc. Am.* 15, 3076
- Baratta, G. A., Leto, G., & Palumbo, M. E. 2002, *A&A*, 384, 343
- Bennett, C. J., Jamieson, C., Mebel, A. M., & Kaiser, R. I. 2004, *Phys. Chem. Chem. Phys.*, 6, 735
- Boland, W., & de Jong T. 1982, *ApJ*, 261, 110
- Bottinelli, S., Ceccarelli, C., Williams, J. P., & Lefloch, B. 2007, *A&A*, 463, 601
- Bringa, E. M., & Johnson, R. E. 2004, *ApJ*, 603, 159
- Brown, R. D., Eastwood, F. W., Elmes P. S., & Godfrey, P. D. 1983, *J. Am. Chem. Soc.*, 105, 6496
- Brown, R. D., Godfrey, P. D., Cragg, D. M., et al. 1985, *ApJ*, 297, 302
- Chiar, J. E., Adamson, A. J., Kerr, T. H., & Whittet, D. C. B. 1994, *ApJ*, 426, 240
- Chiar, J. E., Adamson, A.J., Kerr, T. H., & Whittet, D. C. B. 1995, *ApJ*, 455, 234
- Chiar, J. E., Gerakines, P. A., Whittet, D. C. B., et al. 1998, *ApJ*, 498, 716
- Comoretto, G., Palagi, F., & Cesaroni, R. 1990, *A&AS*, 84, 179
- Crovisier, J., Encrenaz, T., & Combes M. 1991, *Nature*, 353, 610
- Ehrenfreund, P., Boogert, A. C. A., Gerakines, P. A., Tielens, A. G. G. M., & van Dishoeck, E. F. 1997, *A&A*, 328, 649
- Elias, J. H., 1978, *ApJ*, 224, 857
- Ford, K. E. S., Neufeld, D. A., Goldsmith, P. F., & Melnick, G. J. 2003, *ApJ*, 589, 430
- Ford, K. E. S., Neufeld, D. A., Schilke, P., & Melnick, G. J. 2004, *ApJ*, 614, 990
- Fraser, H. J., Collings, M. P., Dever, J. W., & McCoustra, M. R. S. 2004, *MNRAS*, 353, 59
- Gerakines, P. A., Schutte, W. A., & Ehrenfreund, P. 1996, *A&A*, 312, 289
- Gerakines, P. A., Whittet, D. C. B., Ehrenfreund, P., et al. 1999, *ApJ*, 522, 357
- Gerakines, P. A., & Moore, M. H. 2001, *Icarus*, 154, 372

- Goldsmith, P. F., & Langer, W. D. 1999, *ApJ*, 517, 209
- Guelin, M., Langer, W. D., & Wilson, R. W. 1982, *A&A*, 107, 107
- Hasegawa, T. I., & Herbst, E. 1993, *MNRAS*, 261, 83
- Hasegawa, T. I., Kwok, S., Koning, N., et al. 2006, *ApJ*, 637, 791
- Huntress, W. T., Allen, M., & Delitsky, M. 1991, *Nature*, 352, 316
- Kaifu N., Ohishi M., Kawaguchi K., et al., 2004, *Publ. Astron. Soc. Japan*, 56, 69
- Kerkhof, O., Schutte, W. A., & Ehrenfreund, P. 1999, *A&A*, 346, 990
- Kerr, T. H., Adamson, A. J., & Whittet, D. C. B. 1993, *MNRAS*, 262, 1047
- Ioppolo, S., Palumbo, M. E., Baratta, G. A., & Mennella, V. 2008, *A&A*, submitted
- Loeffler, M. J., Baratta, G. A., Palumbo, M. E., Strazzulla, G., & Baragiola, R. 2005, *A&A*, 435, 587
- Matthews, H. E., Irvine, W. M., Friberg, P., Brown, R. D., & Godfrey, P. D. 1984, *Nature*, 310, 125
- Melnick, G. J., Neufeld, D. A., Ford, K. E. S., Hollenbach D. J., & Ashby M. L. N. 2001, *Nature*, 412, 160
- Mennella, V., Baratta, G. A., Esposito, A., Ferini, G., & Pendleton, Y.J. 2003, *ApJ*, 587, 727
- Mulas, G., Baratta, G. A., Palumbo, M. E., & Strazzulla, G. 1998, *A&A*, 333, 1025
- Nummelin, A., Whittet, D. C. B., Gibb, E. L., Gerakines, P. A., & Chiar, J. E. 2001, *ApJ*, 558, 185
- Ohishi, M., Suzuki, H., Ishikawa, S., et al., 1991, *ApJ*, 380, L39
- Palumbo, M. E., & Strazzulla, G. 1993, *A&A*, 269, 568
- Palumbo, M. E., Ferini, G., & Baratta, G. A. 2004, *Adv. Space Res.* 33, 49
- Palumbo, M. E., Baratta, G. A., Brucato, J. R., Castorina, A. C., Satorre, M. A., & Strazzulla, G. 1998, *A&A* 334, 247
- Park, I. H., Wakelam, V., & Herbst, E. 2006, *A&A*, 449, 631

- Pontoppidan, K. M., Fraser, H. J., Dartois, E. et al., 2003, *A&A*, 408, 981
- Shuping, R. Y., Chiar, J. E., Snow, T. P., & Kerr, T. 2001, *ApJ*, 547, L161
- Strazzulla, G., & Johnson, R. 1991, in *Comets in the post Halley era*, ed. R. L. Newburn & M. Neugebauer (Kluwer, Dordrecht) 243
- Strazzulla, G., Baratta, G. A., & Palumbo, M. E. 2001, *Spectrochim. Acta A*, 57, 825
- Strazzulla, G., Brucato, J. R., Palumbo, M. E., & Satorre, M. A. 1997, *A&A*, 321, 618
- Tegler, S. C., Weintraud, D. A., Rettig, T. W., Pendleton, Y. J., Whittet, D. C. B., & Kulesa, C. A. 1995, *ApJ*, 439, 279
- Teixeira, T. C., & Emerson, J. P. 1999, *A&A*, 351, 292
- Teixeira, T. C., Emerson, J. P., & Palumbo, M. E. 1998, *A&A*, 330, 711
- Tenenbaum, E. D., Aponi, A. J., Ziurys, L. M., Agundez, M., Cernicharo, J., Pardo, J. R., Guelin, M., 2006, *ApJ*, 649, L17
- Tielens, A.G.G.M., & Allamandola, L. J. 1987, in: G. E. Morfill, & M. Scholer (eds.), *Physical processes in interstellar clouds*, (Reidel, Dordrecht) p.333
- Tielens, A.G.G.M., Tokunaga, A. T., Geballe, T. R., & Baas, F. 1991, *ApJ*, 381, 181
- Trigilio, C., Umana, G., Siringo, C., Buemi, C., Leto, P., Codella, C., & Panella, D. 2006, *MSAIS* 10, 171
- Trigilio, C., Palumbo, M. E., Siringo, C., & Leto, P. 2007, *ApSS*, in press
- Trottier, A., & Brooks, R. L., 2004, *ApJ*, 612, 1214
- Ziegler, J. F. 2003, *Stopping and Range of Ions in Matter SRIM2003* (available at www.srim.org)

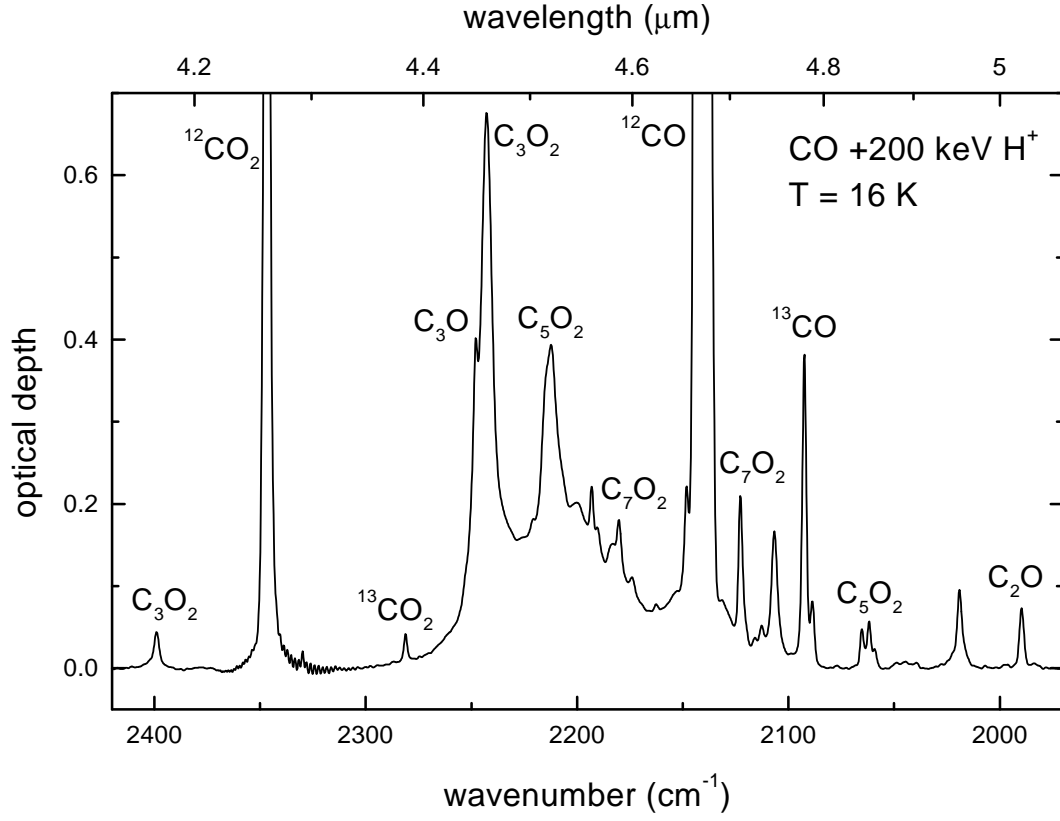


Fig. 1.— Infrared transmission spectrum, in optical depth scale, of CO ice after ion irradiation with 200 keV H⁺ (fluence = 1.25×10^{14} ions cm⁻²) at 16 K. Labels indicate main species present after irradiation.

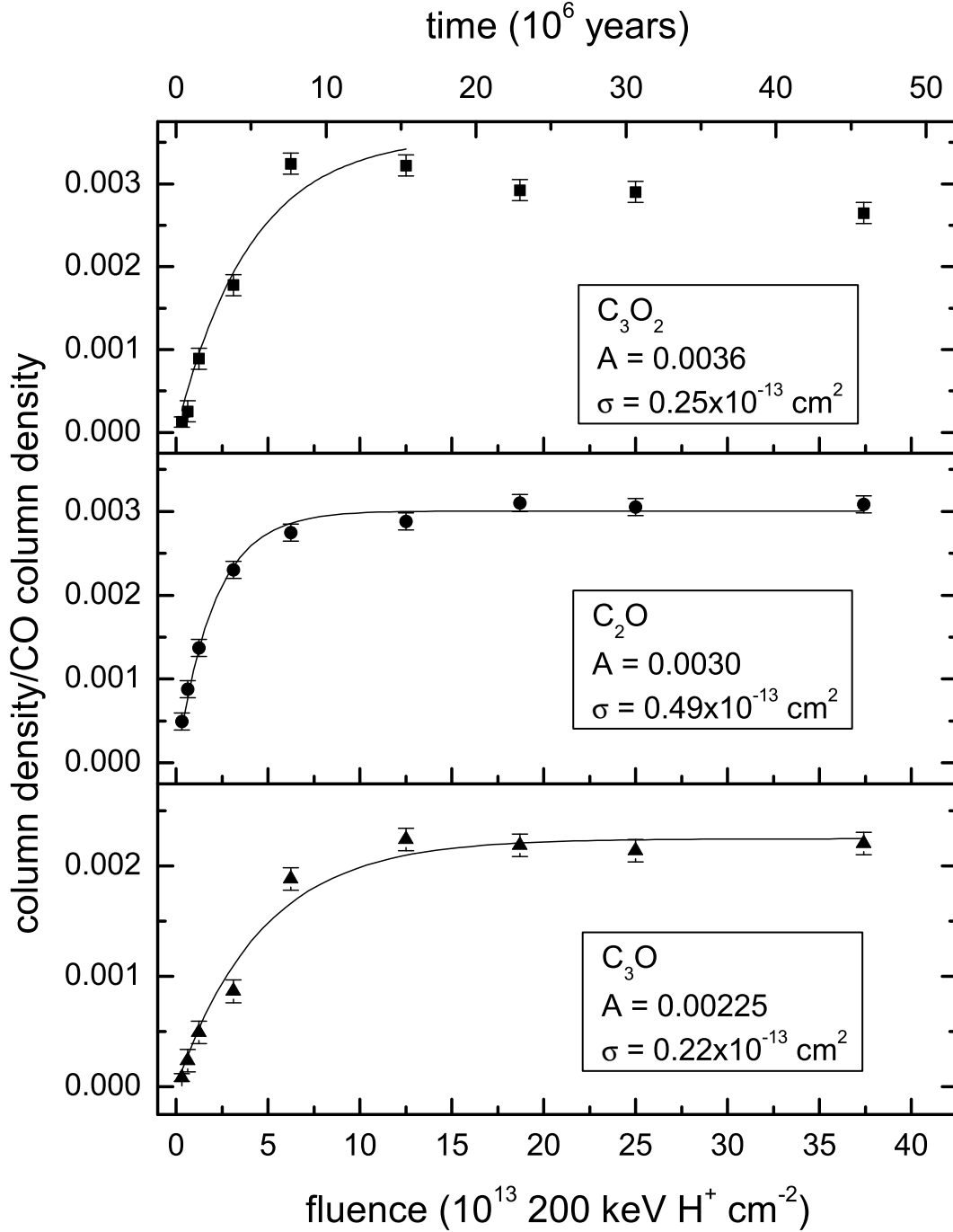


Fig. 2.— Column densities of C_3O_2 , C_2O and C_3O with respect to column density of initial CO as a function of fluence after ion irradiation of pure CO at 16 K with 200 keV H^+ . Top x-axis indicate the time (years) which would be necessary to obtain in dense molecular clouds the same effects observed in laboratory. The experimental data have been fitted with an exponential curve (solid lines) and the fit parameters for each species are reported.

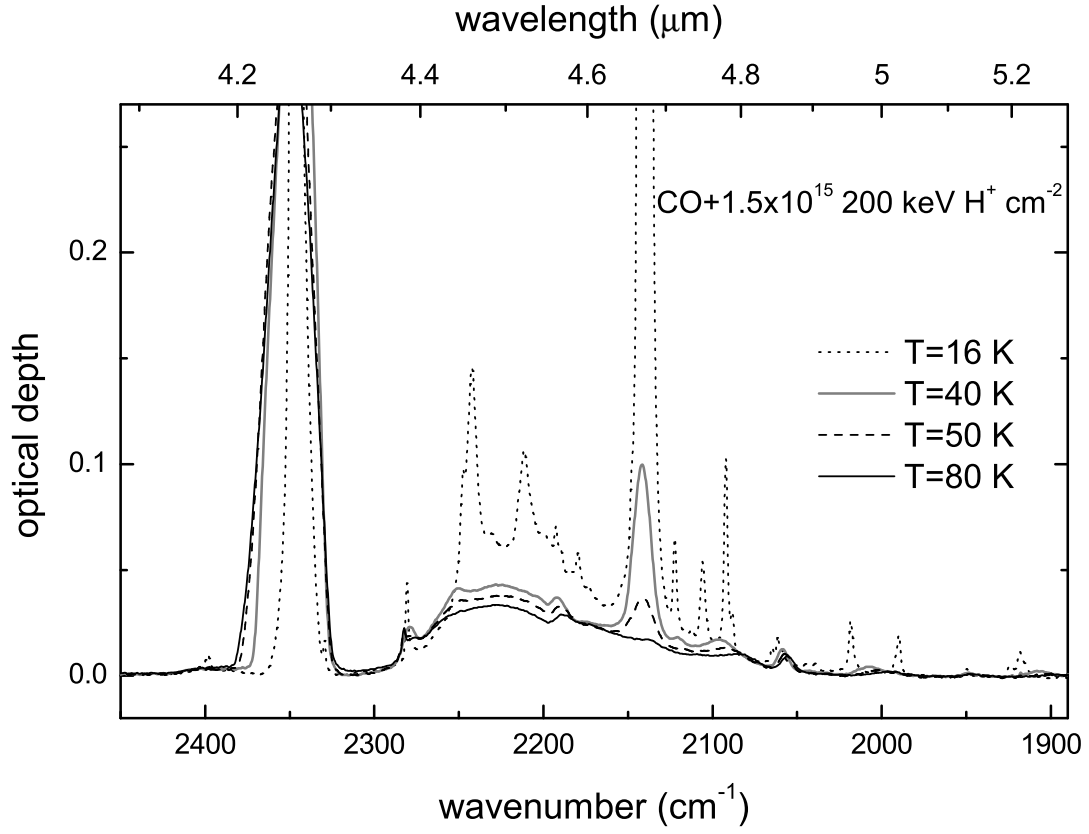


Fig. 3.— Infrared transmission spectra, in optical depth scale, of CO ice after ion irradiation with 200 keV H⁺ (fluence = 1.5×10^{15} ions cm⁻²). Spectra taken at 16 K and after warm up are shown.

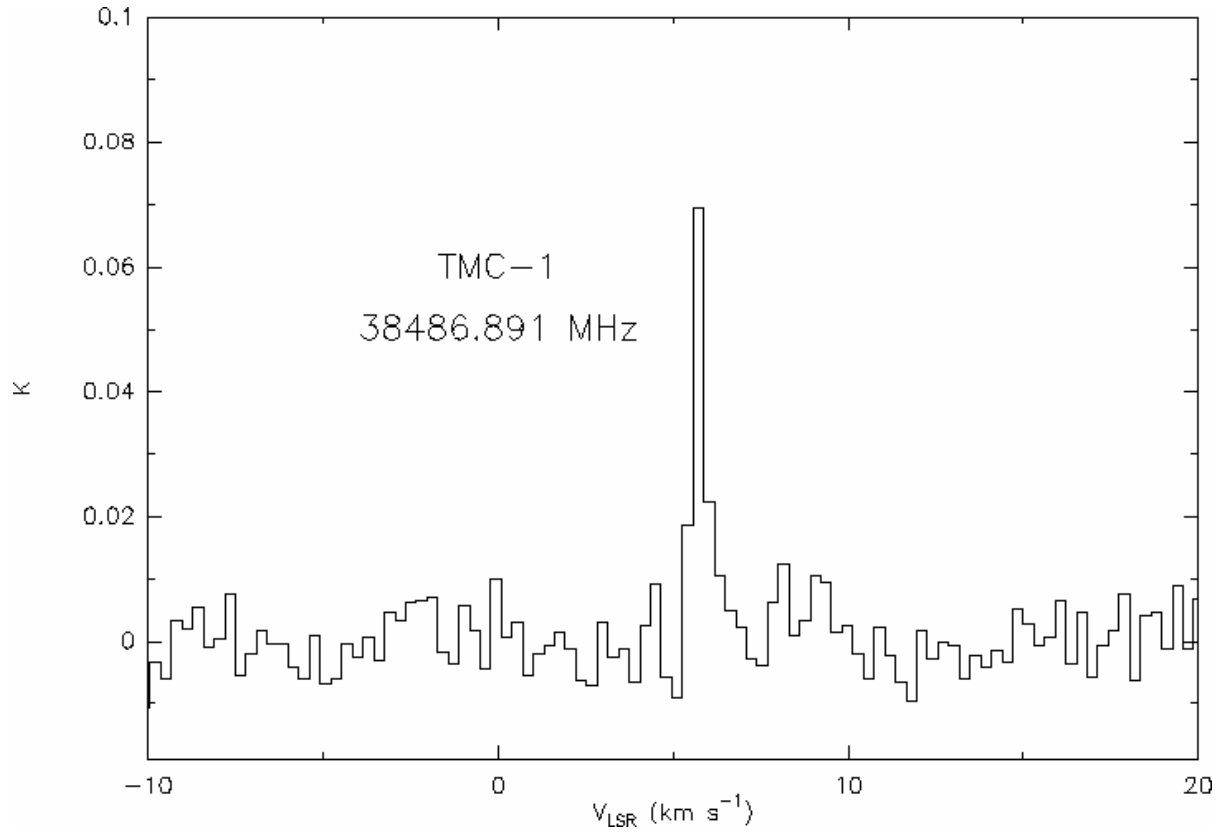


Fig. 4.— C_3O line at 38486.891 MHz detected towards TMC-1CP.

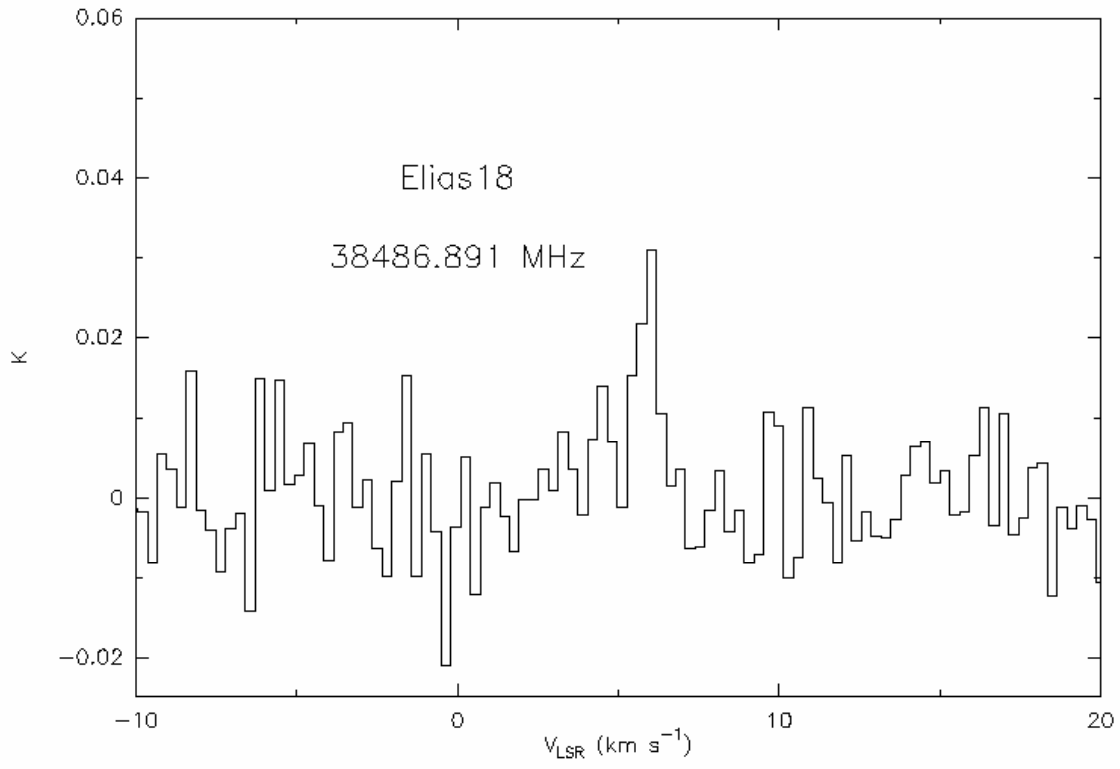


Fig. 5.— C_3O line at 38486.891 MHz detected towards Elias 18.

Table 1: Most intense features detected after irradiation with 200 keV H^+ ions of CO ice at 16 K and their identification.

band position (cm^{-1})	identification
3706	CO_2
3601	CO_2
3069	C_3O_2
2398	C_3O_2
2340	CO_2
2329	$\text{C}^{16}\text{O}^{18}\text{O}$
2280	$^{13}\text{CO}_2$
2247	C_3O
2242	C_3O_2
2211	C_5O_2
2192	OCC^{13}CO
2179	C_7O_2
2140	CO
2122	C_7O_2
2112	C^{17}O
2105	
2092	^{13}CO
2088	C^{18}O
2064	
2061	C_5O_2
2018	
1989	C_2O
1924	
1918	C_4O
1042	O_3

Table 2: Low-mass young stellar objects observed.

Object ^a	Region	$\alpha(2000)$	$\delta(2000)$
TMC-1CP	Taurus	04 41 45.9	25 41 27
TMC1-A	Taurus	04 39 35.0	25 41 47
Elias 18	Taurus	04 39 55.7	25 45 02
L1551 IRS5	Taurus	04 31 33.9	18 08 08
L1489IR	Taurus	04 04 43.1	26 18 58
Elias 29 (WL15)	Ophiuchus	16 27 09.3	-24 37 21
Elias 32 (VS18)	Ophiuchus	16 27 28.5	-24 27 17
WL5	Ophiuchus	16 27 18.0	-24 28 52
CK1 (SVS20)	Serpens	18 29 57.5	01 14 07
SVS4	Serpens	18 29 57.8	01 12 48

^aOther ID is given in brackets.

Table 3: Observation log and rms measured.

Source	CCO		CCO		C ₃ O	
	$\nu=22258.181$ MHz		$\nu=45826.706$ MHz		$\nu=38486.891$ MHz	
	J _N =2 ₁ -1 ₀		J _N =3 ₂ -2 ₁		J=4-3	
	int. time (min)	rms (K)	int. time (min)	rms (K)	int. time (min)	rms (K)
TMC-1CP	300	0.008	140	0.011	380	0.005
TMC-1A					160	0.010
Elias 18	180	0.010	140	0.008	200	0.007
L1551 IRS5	300	0.007	150	0.009	300	0.007
L1489IR	300	0.008	220	0.001	240	0.008
Elias 29	90	0.016	90	0.019	200	0.008
Elias 32	90	0.016	90	0.022	160	0.011
WL5	90	0.018	80	0.025	160	0.009
CK1	120	0.013	120	0.014	230	0.006
SVS4-4	200	0.011	120	0.015	160	0.008